Electron Plasma-Wave Production by Stimulated Raman Scattering: Competition with Stimulated Brillouin Scattering

C. J. Walsh,[a] D. M. Villeneuve, and H. A. Baldis
Division of Physics, National Research Council, Ottawa, Ontario K1A 0R6, Canada
(Received 9 February 1984)

We have used temporally and spectrally resolved Thomson scattering in a CO_2-laser–plasma interaction experiment to identify electron plasma waves driven by stimulated Raman scattering in a low-density preformed plasma. Plasma waves were observed in a Gaussian-shaped plasma whose peak density was in the range $(0.01–0.05)\,n_c$, in qualitative agreement with threshold calculations using a convective amplification model. The plasma waves were observed only during the early part of the pump pulse, and disappeared coincidentally with the onset of ion waves driven by stimulated Brillouin scattering.

PACS numbers: 52.40.Db, 52.25.Gj, 52.35.Py

Stimulated Raman scattering[1–3] (SRS) is one of the two stimulated scattering processes encountered in laser-plasma interactions, the other being stimulated Brillouin scattering (SBS). In the SRS instability, electron plasma waves (EPW's) are resonantly generated by a ∇E^2 ponderomotive force, which itself is produced from the superposition of an ingoing electromagnetic (EM) wave and an outgoing (scattered) EM wave. A resonant interaction occurs for waves satisfying $\omega_0=\omega_s+\omega_{\rm EPW}$, $\vec{k}_0=\vec{k}_s+\vec{k}_{\rm EPW}$ (subscripts 0 and s refer to the pump and scattered EM waves; $\vec{k}$ is the wave number). For low-density plasma, $\vec{k}_{\rm EPW}\approx 2\vec{k}_0$.

Our experiments to study SRS were carried out in two plasma geometries, to enable a comparison to be made with threshold calculations (Fig. 1). In one geometry, a CO_2 laser (used as the EM pump) sees an exponential density profile, $n_e(x)=n_0\exp(-x/L_e)$, and in the other it sees a Gaussian density profile, $n_e(x)=n_0\exp(-x^2/L_g^2)$. The plasma was formed independently of the pump laser by focusing the output of a second Q-switched laser ($\lambda=1.06$ μm) onto a carbon target. The CO_2 laser (1 nsec full width at half maximum, 35 J maximum energy, and $I\leq 2\times10^{14}$ W/cm^2) irradiated the plasma about 10 nsec after the peak of the Q-switched pulse. The peak density seen by the CO_2 laser in the Gaussian geometry could be varied by raising or lowering the target.[4] It was found from interferometry that L_g ranged from 1000 μm at $n_0=0.05\,n_c$ to $L_g\approx 550$ μm at $n_0=0.2\,n_c$, and that $L_e\approx 300$ μm over all densities of interest.

To study the enhancement of the EPW's by SRS during this interaction, we used time- and frequency-resolved Thomson scattering with a 0.53-μm probe pulse. The geometry shown in Fig. 2 was assembled to observe these EPW's, which have $\vec{k}_{\rm EPW}\approx(1-2)\vec{k}_0$. The scattered probe light was dispersed in a spectrograph and imaged into an Imacon 500 streak camera.[5] The spectrum consisted of an ion feature due to SBS with $\Delta\omega\approx 0$, and two electron satellites with $\Delta\omega=\mp\omega_{\rm EPW}$ corresponding to electron plasma waves traveling parallel and antiparallel to k_0; the red-shifted satellite, cor-

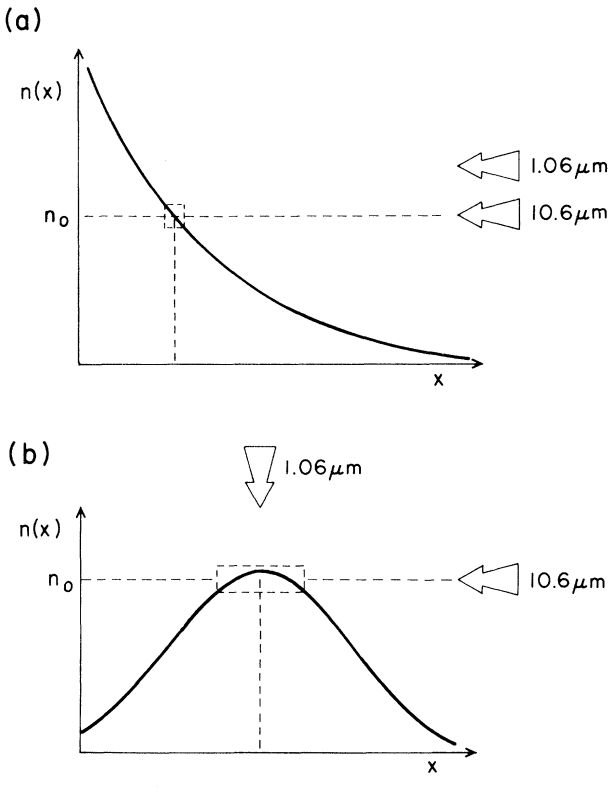

FIG. 1. Diagram of the relative angles of incidence of the 1.06-μm laser pulse (which forms the plasma) and the 10.6-μm laser pulse, and the resulting density profile seen by the CO_2 laser. In the exponential geometry (a), moving the target backward or forward changes the plasma density n_0 in the scattering volume. In the Gaussian geometry (b), scattering observations are always made at the point of maximum density.

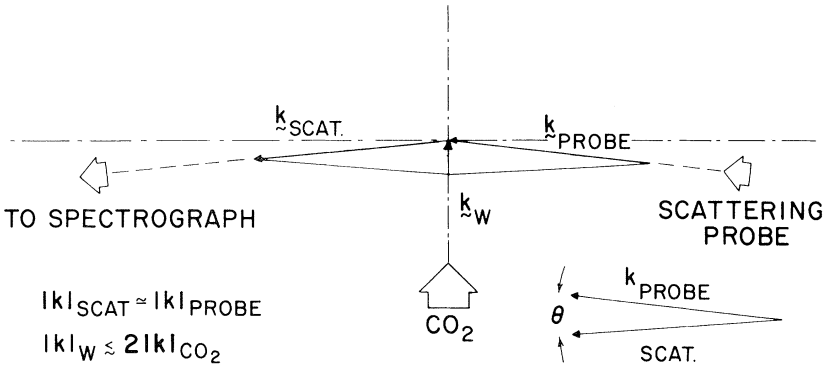

FIG. 2. Diagram of the scattering geometry used. The angle between k_{scat} and k_{probe} is 6° when k_w, the wave vector being probed, is equal to $2k_0$. Electron plasma waves traveling parallel to the pump were selected by setting the spectrograph to the red-shifted electron satellite.

responding to the same direction as k_0, was used. In addition, since the ion feature was much stronger than the electron feature, a block was placed in front of the $\Delta\omega \approx 0$ region. The signal which leaked through the block was used as a fiducial for SBS.[6]

Our experiments in the two geometries yielded the following results. The Raman instability at $n_e \approx n_c/4$ was observed in *both* geometries,[7] whereas the instability at $n_e < n_c/4$ was *only* seen in the Gaussian geometry, and then only at densities between $0.01\,n_c$ and $0.05\,n_c$.

The data to be discussed here concern the observations of SRS at densities $< n_c/4$ in the Gaussian geometry. Since the peak plasma density was less than $n_c/4$, the two-plasmon decay instability was not driven. Some examples of the data are shown in Fig. 3. It can be seen that the EPW's exist for only a short period of time, right at the beginning of the pump pulse, and disappear as the strong ion waves driven by SBS become visible. The duration of the EPW's was related to the pump intensity: For higher intensities they lasted a shorter time, with very little overlap with the ion waves. For the lower intensities more overlap was apparent [e.g., Fig. 3(b)].

A direct comparison of the intensity of the light scattered from the EPW's and from the ion waves, together with a previously derived ion wave amplitude[6] of $\tilde{n}/n = (15 \pm 5)\%$, would suggest $\tilde{n}/n \approx 1\%$ for the EPW's, although this is a volume average.

The density at which the plasma waves were generated, as determined by the frequency shift of the electron feature, corresponded roughly to the peak plasma density as measured interferometrically, although at these low densities interferometry with 0.53-μm light is only accurate to within a factor of 2.

No strong intensity dependence was observed for the production of these EPW's. This may be indicative of some saturation mechanism limiting the EPW amplitude. Evidence for SRS was seen at energies down to 6 J ($I = 3\times10^{13}$ W/cm^2), and even at these low energies, the EPW's occurred before the peak of the CO_2 pulse, and disappeared as the SBS-driven waves appeared. Clearly, the SRS instability has a very low threshold in the Gaussian geometry ($< 10^{13}$ W/cm^2) compared to the exponential geometry, where no evidence for SRS was seen below 10^{14} W/cm^2. We note that these observations were corroborated by measurements of the infrared backscattered radiation at wavelengths between 13 and 15 μm; i.e., no backscatter was seen in the exponential geometry whereas it was in the other.

There is some question as to the conditions under which SRS can be an absolute instability. Dubois, Forslund, and Williams[3] claim it to be absolute if the growth region is bounded; however, in addition to a damping condition, the same inhomogeneous threshold condition applies as that of Rosenbluth.[2] So from an experimental point of view, convective and absolute instabilities are indistinguishable. With use of the convective threshold condition, the interaction length l is calculated from[2] the phase-mismatch condition

$$\int_0^l [k_0(x) - k_s(x) - k_{EPW}(x)]\,dx = \tfrac{1}{2},$$

with use of a local linear or quadratic fit to the plasma profile. The intensity threshold for amplification of 500 above noise level (roughly corresponding to the observed level of signal above thermal fluctuation levels) for the exponential profile is

$$I\lambda^2(\mathrm{W}\ \mu\mathrm{m}^2\ \mathrm{cm}^{-2}) = 4.4\times10^{17}(\lambda/L_e),$$

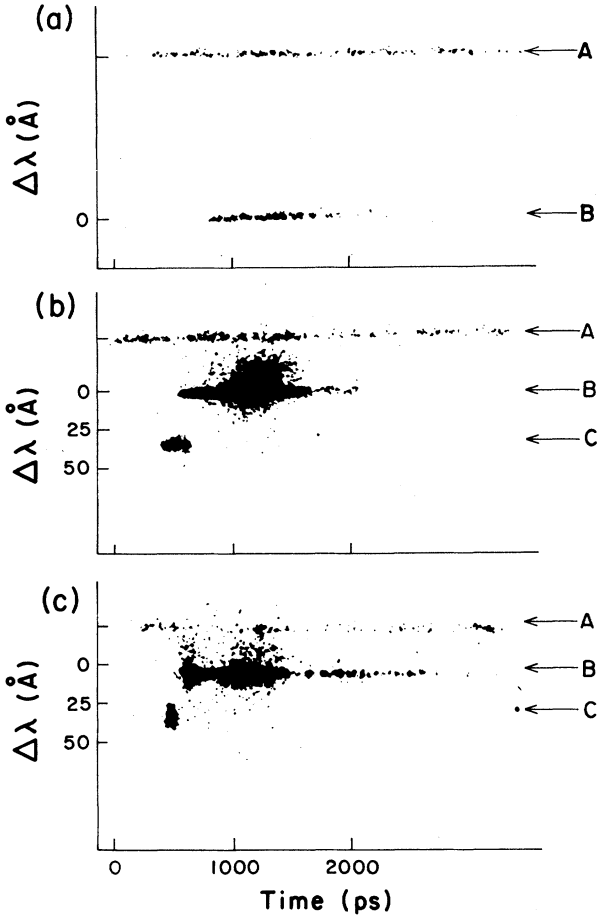

FIG. 3. Three examples of streak data, obtained in the Gaussian geometry. The feature labeled A refers to the monitor of the 0.53-μm probe beam. B refers to the $\Delta\omega \approx 0$ signal, and C refers to the electron satellite due to plasma waves. In (a), the SBS component ($\Delta\omega \approx 0$) is shown (relative attenuation is 500). In (b) and (c), the relative timing between the two components is shown by tuning the spectrograph to allow a small amount of the SBS light to leak past the block. The plasma density corresponding to the wavelength shift of the satellite is given by $n/n_c = 1.4\times10^{-5}(\Delta\lambda)^2$. Plasma waves at $n_c/4$ would produce a shift $\Delta\lambda = 135$ Å. CO_2-laser energies for each shot are (a) 21 J, (b) 11 J, and (c) 34 J.

and for the Gaussian profile is

$$I\lambda^2 = 5.2\times10^{16} T_{\mathrm{keV}}^{1/3} (n_0/n_c)^{-1/3} (\lambda/L_g)^{4/3}.$$

For $T_e = 100$ eV, the thresholds are respectively 1.4×10^{14} and 1.4×10^{12} W/cm^2. These numbers are qualitatively consistent with our observations, since in the Gaussian geometry the threshold was exceeded early in the pulse, but was never exceeded in the exponential geometry.

We now propose a possible explanation for the apparent correlation between the onset of SBS and the disappearance of the EPW's driven by SRS. Rozmus, Offenberger, and Fedosejevs[8] have theoretically considered the SRS process in the presence of ion turbulence driven by SBS. They find that the inhomogeneous SRS threshold condition is modified by the effect of the ion turbulence on the EPW dispersion relation, which becomes $\omega_{\mathrm{EPW}} = \omega_{pe} - \delta\omega_L + 3v_e^2 k_{\mathrm{EPW}}^2/2\omega_{pe}$, where ω_{pe} is the plasma frequency, v_e is the electron thermal velocity, and $\delta\omega_L$ is the frequency shift due to the ion waves.

In order to estimate the effect of ion turbulence on our SRS threshold, we use the example quoted by Rozmus, Offenberger, and Fedosejevs and apply it to our case. The parameters they chose are $T_e = T_i = 45$ eV, $n_0/n_c = 0.027$, and an ion fluctuation level of $\tilde{n}/n = 0.01$ generated by SBS; these are quite close to our parameters.

They assume that the ion fluctuation level decreases with density, so that $\delta\omega_L(x) \sim \delta\omega_L(1 - x/L_H)$, where L_H is the scale length for the fluctuation level. Including this in the phase-mismatch integral leads to the intensity threshold being multiplied by a factor of $(1-\alpha)^{-1}$, where α is a function of $\delta\omega_L$ and the damping rate of the ion waves. They calculate that $\alpha \approx -1$ and thus the SRS threshold will be reduced by a factor of 2.

For the present case, since the SBS growth rate increases with density, we expect the ion fluctuation level to be greatest at the top of the plasma profile. Thus $\delta\omega_L$ increases with increasing plasma density, i.e., $\delta\omega_L(x) = \delta\omega_L(1 + x/L_H)$. The use of the theory of Ref. 8 with the sign of L_H reversed leads to a reversal in the sign of α in the threshold above. For similar plasma parameters, this theory now predicts a significant increase in SRS threshold. For this particular case $\alpha \approx +1$, and the threshold approaches infinity.

Although the numbers may be rough, this calculation illustrates how ion turbulence can interfere with the phase-matching requirements for SRS, and that it is much easier to disrupt SRS (our case) than it is to enhance it[9] (the case of Ref. 8) with the same level of ion fluctuations. This effect of SBS on SRS may have been seen in simulations,[10] where a reduction in the SRS absorption and electron temperature was observed with mobile ions as compared with fixed ions.

Why were plasma waves observed only in the density range $(0.01\text{–}0.05)\,n_c$? Landau damping will limit the growth at low densities as the Debye length λ_D increases. The intensity at which the homogeneous SRS growth rate exceeds the Landau

damping rate is a strong function of density and temperature (electron-ion collisions are negligible). For $n=0.01n_c$ and $T=100$ eV, it increases to over 10^{14} W/cm^2; therefore as the plasma becomes hotter we expect the instability to be strongly damped at lower densities. The data confirm this, showing a trend towards higher plasma-wave frequency with increasing laser intensity. Thus the fact that $k\lambda_D > 0.3$ when $n < 0.01n_c$ and $T=100$ eV explains the low-density cutoff in the signal.

There is a possibility that the detrimental effect of SBS on SRS which is so obvious at the lower densities may also account for the absence of EPW's driven by SRS at the higher densities. The SBS growth rate increases with density (for densities $<0.3n_c$) and the calculations of the SRS growth rate above show it to decrease with increasing density as a result of the decrease in L_g. Thus the competition seen in Fig. 3, which limits the duration of the EPW's at the lowest densities to <200 psec in general, will become dominated by SBS at the higher densities, and SRS may never appear.

To summarize, a model for convective amplification of EPW's driven by SRS appears to explain successfully most aspects of our Thomson-scattering observations in two geometries, and we have clear evidence that under some conditions, ion waves from SBS can quench or inhibit the production of EPW's at $n_e < n_c/4$.

We would like to acknowledge valuable discussions with W. Rozmus, and the technical support of R. Benesch and A. Avery.

---

[a]Present address: Division of Applied Physics, Commonwealth Scientific and Industrial Research Organization, Lindfield, New South Wales 2070, Australia.

[1]J. F. Drake, P. K. Kaw, Y. C. Lee, G. Schmidt, C. S. Liu, and M. N. Rosenbluth, Phys. Fluids **17**, 778 (1974); D. W. Forslund, J. M. Kindel, and E. L. Lindman, Phys. Fluids **18**, 1002 (1975).

[2]M. N. Rosenbluth, Phys. Rev. Lett. **29**, 565 (1972).

[3]D. F. Dubois, D. W. Forslund, and E. A. Williams, Phys. Rev. Lett. **33**, 1013 (1974).

[4]H. A. Baldis and C. J. Walsh, Phys. Fluids **26**, 1364 (1983).

[5]H. A. Baldis, C. J. Walsh, and R. Benesch, Appl. Opt. **21**, 297 (1982).

[6]C. J. Walsh and H. A. Baldis, Phys. Rev. Lett. **48**, 1483 (1982).

[7]D. M. Villeneuve, C. J. Walsh, and H. A. Baldis, to be published.

[8]W. Rozmus, A. A. Offenberger, and R. Fedosejevs, Phys. Fluids **26**, 1071 (1983).

[9]A. A. Offenberger, R. Fedosejevs, W. Tighe, and W. Rozmus, Phys. Rev. Lett. **49**, 371 (1982).

[10]K. Estabrook and W. L. Kruer, Phys. Fluids **26**, 1892 (1983).